

EXPERIMENTAL STUDY ON THE EFFECT OF MISFIT AND MISMATCH OF
SHIP PLATING WELDS

by

Robert E. Bebermeyer

DISTRIBUTION STATEMENT A

Approved for Public Release

Distribution Unlimited

B.S., Electrical Engineering, Michigan State University, 1992
M.S., Electrical Engineering, Michigan State University, 1993

SUBMITTED TO THE DEPARTMENT OF OCEAN ENGINEERING AND THE
DEPARTMENT OF MECHANICAL ENGINEERING
IN PARTIAL FULFILLMENT OF THE REQUIREMENTS FOR THE DEGREES OF

NAVAL ENGINEERS DEGREE

and

MASTER OF SCIENCE IN MECHANICAL ENGINEERING

At the
MASSACHUSETTS INSTITUTE OF TECHNOLOGY
June 2002

©2002 Massachusetts Institute of Technology. All rights reserved.

Signature of Author.....

Robert E. Bebermeyer
Department of Ocean Engineering and
The Department of Mechanical Engineering

16 May 2002

Certified by.....

Tomasz Wierzbicki
Tomasz Wierzbicki
Professor of Applied Mechanics
Thesis Supervisor

Certified by.....

Frank A. McClintock
Frank A. McClintock
Professor of Mechanical Engineering
Thesis Reader

Accepted by.....

Ain A. Sonin
Professor Ain A. Sonin
Chairperson, Department Committee on Graduate Students
Department of Mechanical Engineering

Accepted by.....

Henrik Schmidt
Professor Henrik Schmidt
Professor of Ocean Engineering
Chairperson, Department Committee on Graduate Students

20020822 005

**Experimental Study on the Effect of Misfit and Mismatch of
Ship Plating Welds**

by

Robert E. Bebermeyer

Submitted to the department of Ocean Engineering and the
Department of Mechanical Engineering
on 16 May 2002, in partial fulfillment of the
requirements for the degrees of

Naval Engineers Degree

and

Master of Science in Mechanical Engineering

ABSTRACT

Misfits and mismatches in the welding of ship hull plating may affect survivability after explosions, accidents, or other extreme external forces. Experiments, Slip Line Theory (SLT), and Finite Element Analysis (FEA) help to explain the necking, deformation, and mechanisms of fracture of misfit welded plating. The effect of misfits or offsets on both overmatched and evenmatched welds under tension are studied. The tension creates a moment about the offset weld causing the weld to rotate and the material around the weld to thin down, but strain hardening reduces the thinning that occurs and shifts deformation elsewhere away from the weld.

EH-36, a commercial medium strength steel now being used in Navy surface combatants, was tested. The overmatched EH-36 misfit welds experienced rotation, minor thinning near the weld, and deformation elsewhere as predicted.

AL6XN, a new stainless steel with evenmatched welds, gave nearly the same results as the EH-36. There was a 3% reduction in maximum applied force per area for the 30% offset case, and an increase in the amount of thinning near the weld.

Thesis Supervisor: Tomasz Wierzbicki
Title: Professor of Applied Mechanics

Thesis reader: Frank A. McClintock
Title: Professor of Mechanical Engineering

ACKNOWLEDGEMENTS

The author would like to express his appreciation to both of his academic advisors, Professor Tomasz Wierzbicki, of the Department of Ocean Engineering, and Professor Frank McClintock, of the Department of Mechanical Engineering, for all of their support and patience during the completion of this thesis work.

The welding of the EH-36 was done in cooperation with Bath Iron Works. Thanks to the efforts of:

- Dave Forrest, Principal Engineer, Bath Iron Works
- Dean Brown, Welder, Bath Iron Works
- CDR Tim McCoy, Project Officer for LPD 17

The work on the AL6XN would not have been possible without the contribution of time and resources by:

- Steven Miley, Metro Machines
- Jack Bower, Lehigh University
- Dr. Roshdy Barsoum, Office of Naval Research

Finally, I would like to thank my family who gave me the strength, ability, and time to complete my degrees.

Table of Contents

ABSTRACT	2
ACKNOWLEDGEMENTS	3
TABLE OF CONTENTS	4
LIST OF FIGURES.....	6
LIST OF TABLES.....	7
NOMENCLATURE	8
CHAPTER 1 INTRODUCTION.....	9
1.1 NEED FOR THIS RESEARCH	9
1.2 DEFINITION OF PROBLEM.....	9
1.3 PREVIOUS WORK.....	10
1.4 STRUCTURE OF THIS THESIS.....	11
CHAPTER 2 ANALYTICAL AND NUMERICAL MODELING	12
2.1 MODELING OF THE WELD REGION.....	12
2.2 SLIP LINE THEORY	14
2.3 GEOMETRIC MODELING.....	16
2.4 FINITE ELEMENT ANALYSIS	17
CHAPTER 3 EXPERIMENTAL PROCESS	19
3.1 STATEMENT OF PROBLEM.....	19
3.1.1 Boundary Conditions for Service and Testing Conditions.....	19
3.1.2 Evaluating the Service Condition.....	25
3.1.3 Analysis of the Ratio of Shear Force to Tensile Force.....	26
3.2 DESIGN OF SPECIMENS.....	28
3.2.1 Determining Specimen Measurements.....	28
3.3 TESTING OF SPECIMENS.....	32
CHAPTER 4 RESULTS	34
4.1 EXPERIMENT CRITERION	34
4.1.1 Specimen Fabrication.....	34
4.1.2 Testing of the design specimens.....	35
4.2 EXPERIMENTAL RESULTS.....	36
4.2.1 EH-36 Experimental Results.....	36
4.2.2 AL6XN Experimental Results	37
4.2.3 Analysis of Experimental Results	37
CHAPTER 5 DISCUSSION AND CONCLUSIONS.....	44
5.1 DISCUSSION	44
5.2 RECOMMENDATIONS FOR FURTHER STUDY	45
5.3 CONCLUSIONS	46
CHAPTER 6 REFERENCES.....	47

APPENDIX A SPECIMEN CALCULATIONS.....	48
APPENDIX B EH 36 PLATE SPECIMEN TEST DATA	50
APPENDIX C AL6XN PLATE SPECIMEN TEST DATA	51
APPENDIX D BOUNDARY CONDITION CALCULATIONS	52
APPENDIX E SERVICE CONDITION EVALUATION CONDITION	55
APPENDIX F DETERMINING SPECIMENT MEASUREMENTS	57
APPENDIX G DESIGN SCHEMATICS OF TEST SPECIMENS	60
APPENDIX H EH-36 ENGINEERING STRESS VS. GAUGE STRAIN	62
APPENDIX I AL6XN ENGINEERING STRESS VS. GAUGE STRAIN	64

LIST OF FIGURES

FIGURE 1. GENERAL SCHEMATIC FOR NOMENCLATURE	8
FIGURE 2. WELD AND HAZ REGIONS.....	13
FIGURE 3. EH-36 WELD HARDNESS PROFILE [REF]	13
FIGURE 4. STRESS-STRAIN CURVES OF MATERIAL.....	14
FIGURE 5. FREE BODY DIAGRAM OF WELDMENT	15
FIGURE 6. 15% OFFSET WITH SHEAR BANDS FORMING NEAR WELD.....	18
FIGURE 7. FREE BODY DIAGRAM OF CENTER WELD REGION	20
FIGURE 8. IN SERVICE SCHEMATIC	20
FIGURE 9. BEFORE AND AFTER DISPLACEMENT APPLIED TO SERVICE CONDITION.....	21
FIGURE 10. BEFORE AND AFTER DISPLACEMENT APPLIED TO TEST CONDITION	22
FIGURE 11. BEFORE AND AFTER DISPLACEMENT APPLIED TO FREE BODY	26
FIGURE 12. FREE BODY DIAGRAM OF INFINITE TEST CASE.....	27
FIGURE 13. TOP VIEW DRAWING OF SPECIMEN MEASUREMENTS	29
FIGURE 14. MTS TESTING MACHINE WITH SPECIMEN IN GRIPS	35
FIGURE 15. 2D FEA ANALYSIS OF EH36 <u>WITHOUT</u> STRAIN HARDENING (30% OFFSET) ...	38
FIGURE 16. 2D FEA ANALYSIS OF EH36 <u>WITH</u> STRAIN HARDENING (30% OFFSET).....	39
FIGURE 17. 3D FEA MODEL OF EH36 WITH STRAIN HARDENING (30% OFFSET)	40
FIGURE 18. WELD ROTATION VERSUS NORMALIZED ELONGATION OF EH36 (30% OFFSET)	41
FIGURE 19. LOAD PER AREA VS. NORMALIZED ELONGATION OF EH-36. (30% OFFSET)...	42
FIGURE 20. 30% OFFSET CASE	60
FIGURE 21. 15% OFFSET CASE	60
FIGURE 22. 0% OFFSET CASE	61

LIST OF TABLES

TABLE 1. ALLOWABLE BUTT WELD OFFSETS [8]	10
TABLE 2. ASSUMED MATERIAL PROPERTIES FOR ABACUS®	17
TABLE 3. MATERIAL PROPERTIES OF EH 36 AND AL6XN.....	31
TABLE 4. MEASUREMENTS FOR EH 36 AT VARYING OFFSETS.....	32
TABLE 5. MEASUREMENTS FOR AL6XN AT VARYING OFFSETS	32
TABLE 6. SUMMARY OF TEST RESULTS OF EH 36 SPECIMENS	36
TABLE 7. SUMMARY OF TEST RESULTS FOR AL6XN.....	37

NOMENCLATURE

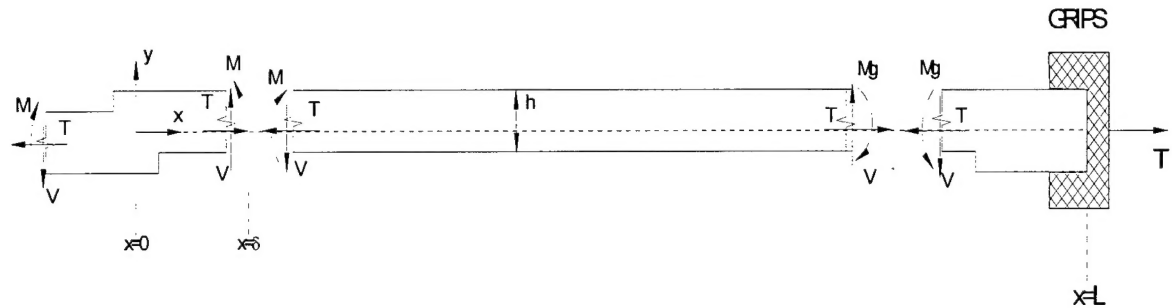


Figure 1. General schematic for nomenclature

Some of the general nomenclature to be used in this paper is,

L = Length of plate from origin to end of plate in x -direction

λ = Wavelength of plate under tension $= \sqrt{EI/T}$

T = Tension force reaction to displacements applied to ends of the plate

V = Shear force in plate

M = Bending moment about the plate

M_g = Bending moment about the plate at the grips

h = plate thickness in y direction

E = Modulus of elasticity of specimen

I = Area moment of inertia of specimen cross section

w = Width of specimen

CHAPTER 1 INTRODUCTION

1.1 NEED FOR THIS RESEARCH

This paper arose from the need to analyze the benefits of precision manufacturing with regards to welding with reduced misfit of ship hull plating. The Office of Naval Research (ONR) has expressed interest in the possible benefits of precision welding as it applies to both mid-grade steels (such as the commercial EH-36 currently being used in the construction of the LPD 17 ship class) as well as new types of stainless steels, in particular AL6XN.

1.2 DEFINITION OF PROBLEM

The problem to be analyzed is concerned with the misfit of ship hull plating when welded. We can analyze the weld region as the hull plates on either side are placed in tensions due to an applied displacement, possibly resulting from an

underwater explosion (UNDEX). The weld region will tend to rotate, based on Slip Line Theory (SLT) [2,7,10] and Finite Element Analysis (FEA), thereby causing the region to neck. The necking region would then have a reduced strength and be more likely to become an area of increased deformation and possible failure. This thesis will look at the forces involved for the misfit of common mild strength steel as well as some newer stainless steels.

The allowable offsets are:

Plate Thickness (in)	Allowable Offset (in)	Allowable Offset %
Less than 3/8	1/16	$\geq 16.67\%$
3/8 to 3/4	1/8	16.67 – 33 %
over 3/4 to 1-1/2	3/16	12.5 – 25 %
over 1-1/2	1/4	$\leq 16.67\%$

Table 1. Allowable butt weld offsets [8]

1.3 PREVIOUS WORK

Previous work on this research was done by Weaver and documented in a thesis titled 'Ship Hull Plating Weld Misalignment Effects when Subjected to Tension' [7]. This thesis showed, using FEA, the importance of a deformed geometry in promoting final fracture by slip from the toe of the weld in non-hardening materials. Graphical results indicated that for a non-hardening material with an

offset of 15% of the plate thickness, weld rotation of 4-6° and local plate thinning of 4-5% in the region next to the weld can be expected. A test specimen with a 15% offset and a simulated weld region, showed a 4°-weld rotation but did not provide the plane-strain condition and failed by necking away from the weld. A redesign of specimens and actual welding of specimens was suggested.

1.4 STRUCTURE OF THIS THESIS

The thesis begins with an introduction explaining the needs for the analysis of welding of misfit ship hull plating. Analysis and numerical modeling of SLT, geometric modeling, and a look at FEA follow next. Then the setup of the experiment and design of the specimen are discussed. This section includes all of the analytical results required to create the experiment. Finally presented is the summary of the results of the experiment and the discussions and conclusions that were found.

CHAPTER 2 ANALYTICAL AND NUMERICAL MODELING

2.1 MODELING OF THE WELD REGION

The U.S. Navy is starting to use commercial grade steel in its new ship designs. One example of this is the use of medium strength commercial steel, EH-36, being used in construction of the new LPD-17 ship class. In over-matched welded joints, the hardness of the weld is greater than the base metal. The region between the weld and the base metal is called the heat-affected zone (HAZ) as shown in Figure 2, where h is the plate thickness and m is the fractional percentage of the offset based on the plate thickness. Being next to the base metal it is cooled rapidly and is usually harder (see Figure 3). It is currently normal ship building practice to use over-matched welds with the EH-36 [9], which allows us to view the weld and HAZ as a rigid body with respect to the

base metal. It is also possible to include the HAZ region as part of the weld region since the HAZ is very small with respect to the thickness of the plating.

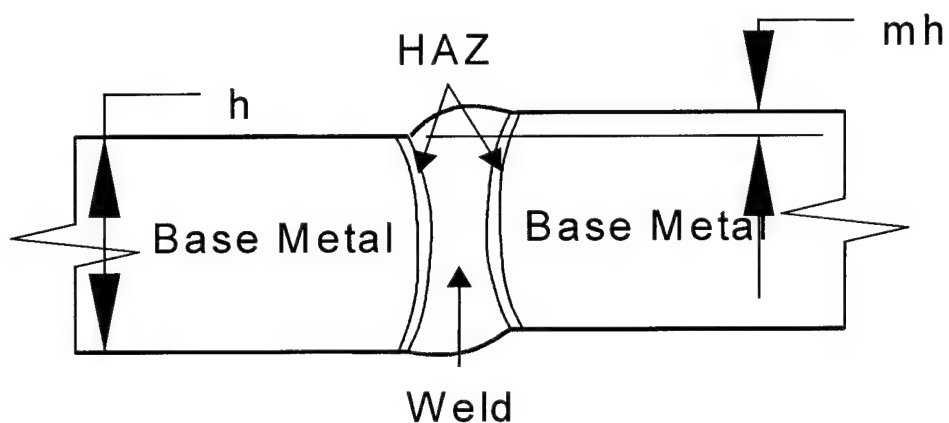


Figure 2. Weld and HAZ regions

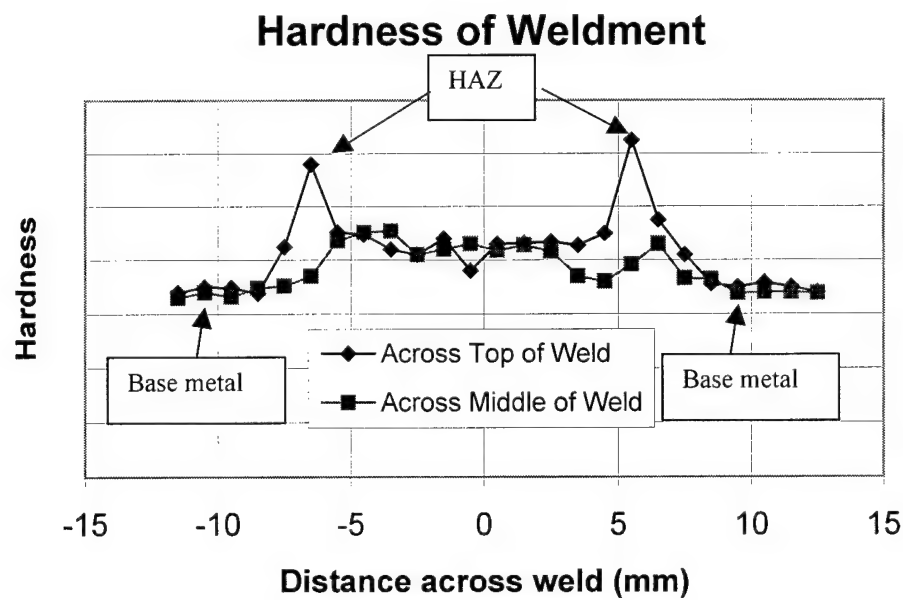


Figure 3. EH-36 weld hardness profile [5]

2.2 SLIP LINE THEORY

During application of slip line theory, we will assume a rigid-perfectly plastic material based on the small fraction of elastic strain that occurs at yield. We can model the stress strain curve as shown in Figure 4.

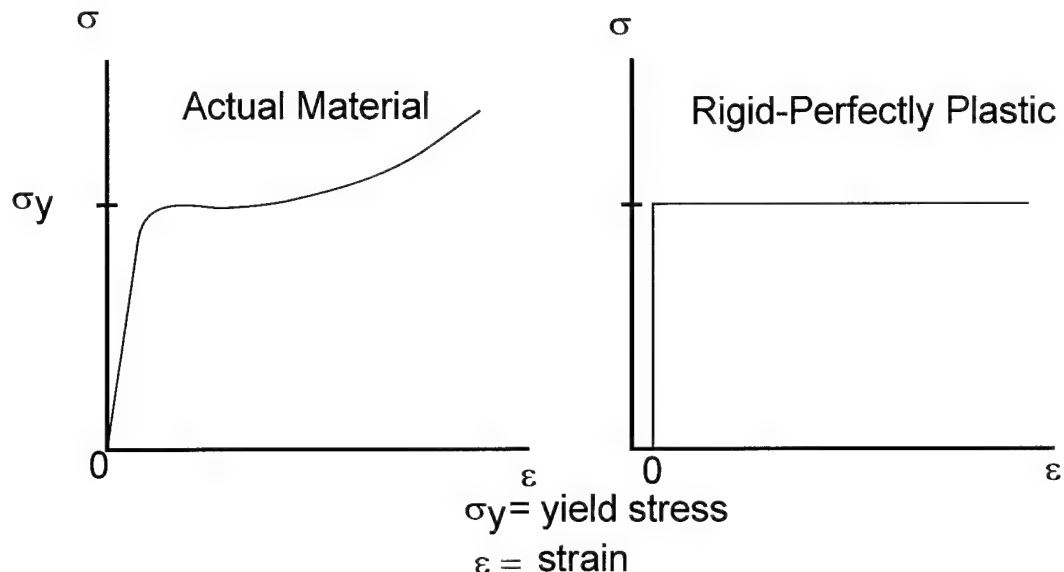


Figure 4. Stress-Strain curves of material

Thus, the following initial assumptions are made:

- Plane strain condition exists
- Elastic-strains neglected (Non-hardening material)
- Rigid-perfectly plastic behavior

It follows from McClintock [2]: a maximum shear stress, k , acts at $+45^\circ$ from the free surface shown. The α and β slip lines are mutually perpendicular curved

lines locally parallel to the directions of the maximum shear stress, such that $\sigma_{\alpha\beta}=k$. They are chosen so that the local direction of maximum principal stress lies 45° counter-clock-wise (ccw) from the α -line toward the β -line. It has also been shown by Weaver [7] that the two active slip line fields approach a neutral axis for welded plates with misfits.

By assuming an applied displacement at the ends of the plates, the problem can be modeled as a far field force P acting through the weld's center. By summing the forces and moments about a point O shown in Figure 5, we arrive at the following equations:

$$\sum F_x = -P + 2k(h - y_{na}) - 2ky_{na} = 0 \quad (2.2.1)$$

$$\sum M_o = -P \left(\frac{1}{2} h + y_p - y_{na} \right) + \frac{1}{2} 2ky_{na}^2 + \frac{1}{2} 2k(h - y_{na})^2 = 0 \quad (2.2.2)$$

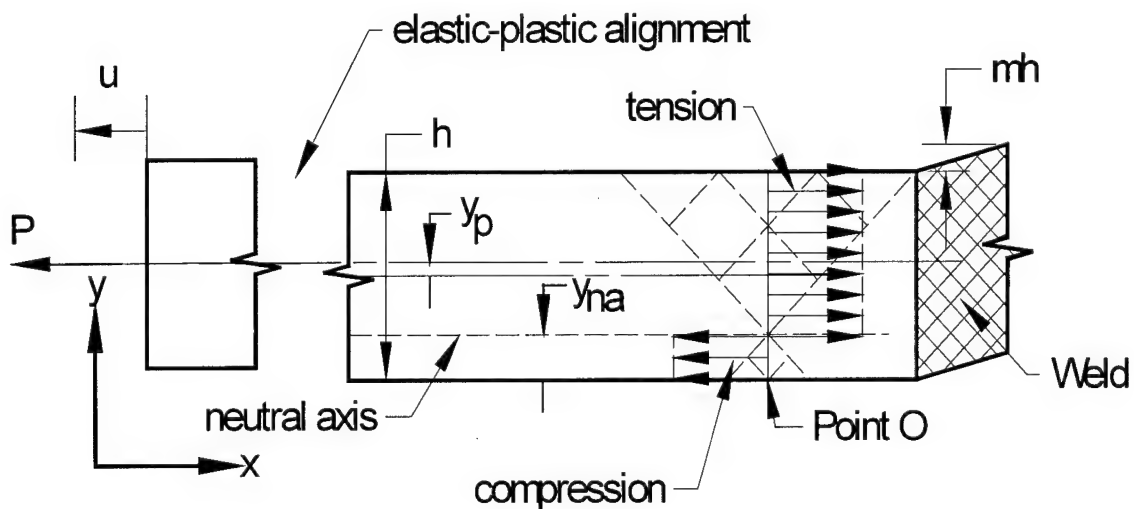


Figure 5. Free Body Diagram of weldment

From this set of equations we can solve for the location of the neutral axis, which ends up being a function of the thickness (h) and the offset (mh). The neutral axis is represented then as:

$$y_{na} = \frac{1}{2} (h + mh - \sqrt{h^2 + m^2h^2}) \quad (2.2.3)$$

Note that this equation is a correction to what was originally presented by Weaver [7].

2.3 GEOMETRIC MODELING

As demonstrated by Weaver [7], the software program DELTACAD[®] was used to provide accurate geometrical and graphical solutions. An applied displacement acts as an externally applied force, P, and the offset of this line of action imposes a moment that tends to rotate the weld. This removes some of the offset, shifting the neutral axis down, and causing the resulting stress components along the rigid body interface closer to a line of action through the center of the weld.

It is assumed the deforming top and bottom surfaces remain straight. However, since the neutral axis is shifting down, the affected top surface becomes longer, resulting in a small curved section at the left end of the slip line field shown. This effect is considered small and negligible.

It is evident that some thinning occurs in the region next to the weld. However, the resulting stresses acting on the interface between the slip line field and the

weld are not yet in equilibrium. The center of the slip line face in the slip field is lower than the center of the weld. Further rotation of the weld is necessary to reach equilibrium.

For an offset of 30%, a weld rotation of 7 degrees is expected, while for an offset of 15%, a weld rotation of 4 degrees is expected.

2.4 FINITE ELEMENT ANALYSIS

Finite element analysis was also conducted on the rigid-perfectly plastic model to verify both the slip line theory and the experimental data. These finite element solutions are based on work done by Teng [6]. The following properties of the base metal and weld metal were initially assumed based on Weaver [7] and Teng [6]:

For EH-36 and AL6XN, we have:

	Base Metal	Weld Metal
Modulus of Elasticity, E	200,000 MPa	200,000 MPa
Upper Yield Point, UYP	200 MPa	260 MPa
Poisons ratio, ν	0.33	0.33

Table 2. Assumed Material Properties for ABACUS®

These values were chosen to mimic a rigid-perfectly plastic, nearly incompressible, model. A displacement was applied at each end of the model while the center of the weld was fixed. The output from the finite element program ABACUS® is shown in Figure 6 for the case of 15% offset. The neutral axis is easily visible as well as the slip line fields and bands of shear.

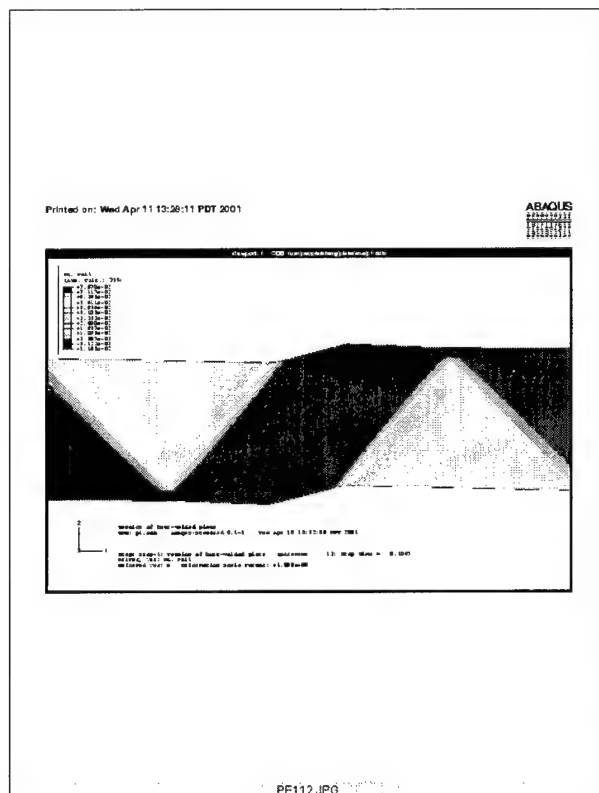


Figure 6. 15% offset with shear bands forming near weld

CHAPTER 3 EXPERIMENTAL PROCESS

3.1 STATEMENT OF PROBLEM

3.1.1 Boundary Conditions for Service and Testing Conditions

Our specimens consist of two pieces of steel that have been welded together with an offset present at the weld. The specimen will then have a displacement applied to each end to test for failure mechanisms. The line of action of the reactionary tension, T , imposes a moment that tends to rotate the weld. This removes some of the offset, shifting the neutral axis down, and causing the resulting stress components along the rigid body of the weld closer to the line of action through the center of the weld. See the free body diagram in Figure 7.

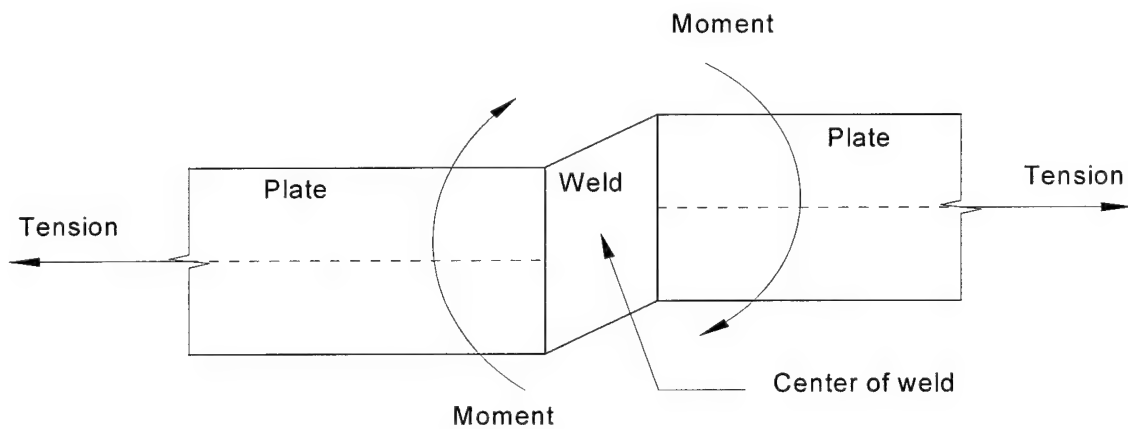


Figure 7. Free Body Diagram of center weld region

We will then need to compare the boundary conditions from the service condition with those from the test condition.

We will start out looking at the in-service schematic in Figure 8.

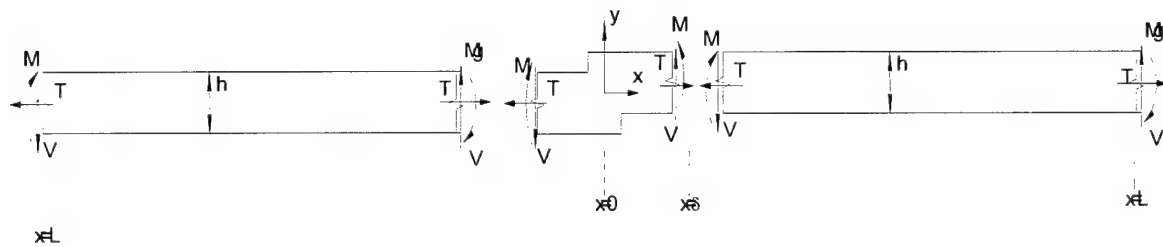


Figure 8. In service schematic

Due to symmetry we can just look at the right half. The figure shows the service condition before and after the displacement is applied as seen in Figure 9. The displacement is represented by the tensile force, T .

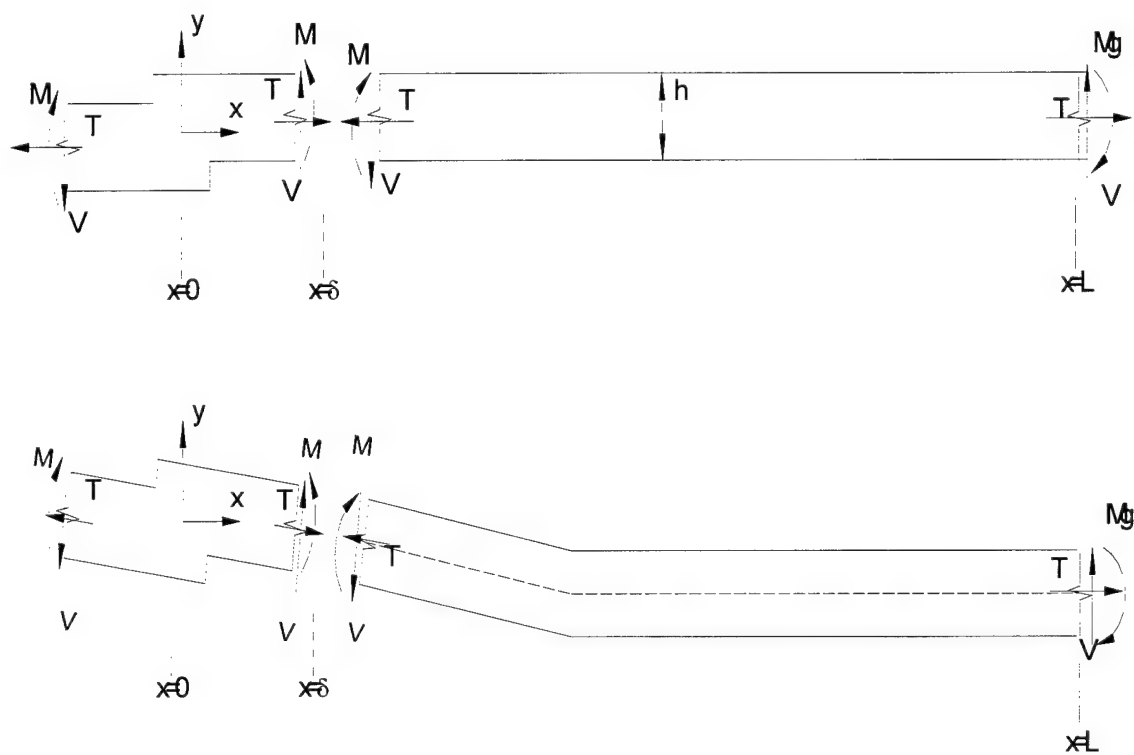


Figure 9. Before and after displacement applied to service condition

The bending shown in figures 9, 10, and 11, is exaggerated here to illustrate the slight bend that will occur as the weld rotates.

The specimen can be seen in the test condition as well. Figure 10 shows both before and after the displacement is applied.

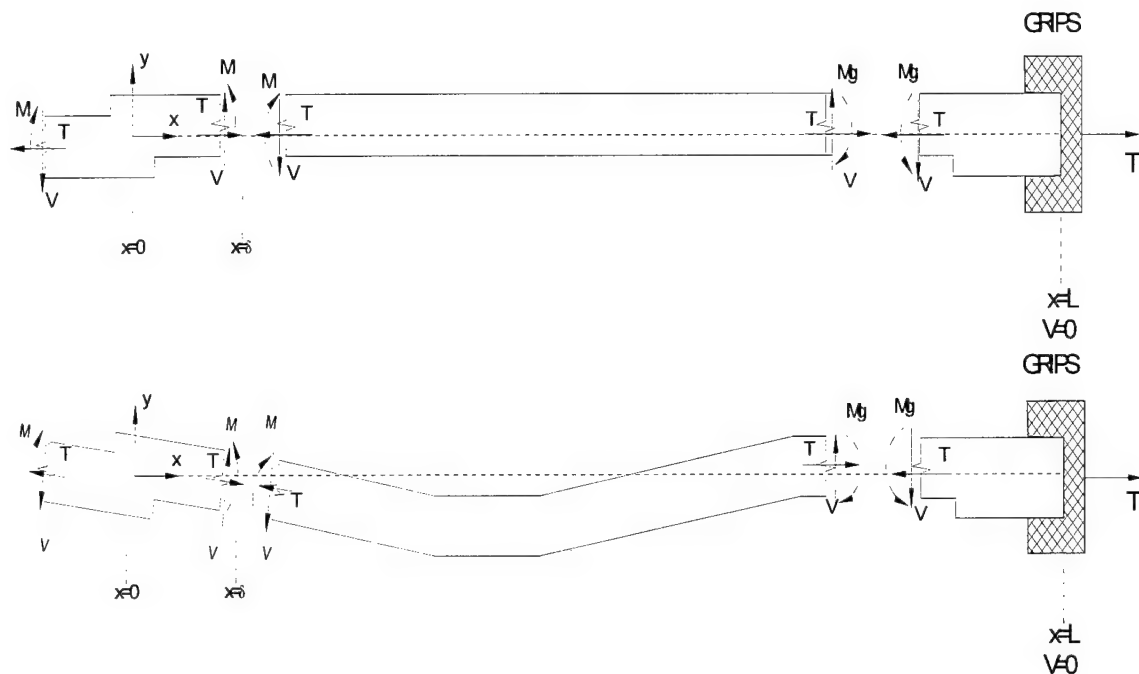


Figure 10. Before and after displacement applied to test condition

The specimen (plate) is under tension (T).

From the analysis of the free body diagram we have the following differential equation [3] for the specimen deflection, $v(x)$, which is:

$$EI \frac{d^4 v(x)}{dx^4} - T \frac{d^2 v(x)}{dx^2} = 0 \quad \text{for} \quad 0 \leq x \leq L \quad (3.1.1)$$

where T is the applied tensile force. The general solution to this differential equation is, in terms of wavelength,

$$\lambda = \left(\frac{EI}{T} \right)^{1/2}, \quad (3.1.2)$$

Given by:

$$v(x) = B_1 + B_2 x + B_3 e^{x/\lambda} + B_4 e^{-x/\lambda} \quad (3.1.3)$$

Four boundary conditions for our specimen are:

At $x=0$:

Bending Moment = Tension * moment arm,

$$EI \frac{d^2 v(x=0)}{dx^2} = T \frac{mh}{2} \quad (3.1.4)$$

Deflection is Maximum at the origin,

$$v(x=0) = v_{\max} = \frac{mh}{2} \quad (3.1.5)$$

At $x=L$:

Zero Deflection at the grips,

$$v(x=L) = 0 \quad (3.1.6)$$

Zero Slope at the grips,

$$\frac{dv(x=L)}{dx} = 0 \quad (3.1.7)$$

From equation (3.1.3) we can calculate the first and second derivatives of the deflection function,

$$\frac{dv}{dx} = B_2 + (1/\lambda) B_3 e^{x/\lambda} + (-1/\lambda) B_4 e^{-x/\lambda} \quad (3.1.8)$$

and,

$$\frac{d^2 v}{dx^2} = (1/\lambda)^2 B_3 e^{x/\lambda} + (-1/\lambda)^2 B_4 e^{-x/\lambda} \quad (3.1.9)$$

Substituting the above quantities into the four boundary conditions, as seen in Appendix D results in:

$$B_3 + B_4 = \frac{mh}{2}$$

$$B_1 + B_3 + B_4 = \frac{mh}{2}$$

$$B_1 + B_2 L + B_3 e^{L/\lambda} + B_4 e^{-L/\lambda} = 0$$

$$B_2 + \frac{1}{\lambda} B_3 e^{L/\lambda} - \frac{1}{\lambda} B_4 e^{-L/\lambda} = 0$$

(3.1.10)

Unknown in equation (3.1.10) are B_1 , B_2 , B_3 , and B_4 , while T , E , I , L , λ , and h are all known or measurable quantities.

This leaves us with **4 equations** and **4 unknowns**, so we can solve for each variable in terms of our known quantities. This can also be done using matrix algebra, math programs such as MathCad, or by hand calculations. The coefficients are,

$$B_1 = \frac{mh}{2}(1-1) = 0$$

$$B_2 = \frac{1}{\lambda} [B_4 e^{-L/\lambda} - B_3 e^{L/\lambda}] = \frac{1}{\lambda} \left[\left(\frac{mh}{2} - B_3 \right) e^{-L/\lambda} - B_3 e^{L/\lambda} \right]$$

$$B_2 = \frac{1}{\lambda} \left[\frac{mh}{2} e^{-L/\lambda} - \frac{\frac{mh}{2} e^{-L/\lambda} (1 + \frac{L}{\lambda})}{e^{L/\lambda} (-1 + \frac{L}{\lambda}) + e^{-L/\lambda} (1 + \frac{L}{\lambda})} (e^{L/\lambda} + e^{-L/\lambda}) \right]$$

$$B_3 = \frac{\frac{mh}{2} e^{-L/\lambda} (1 + \frac{L}{\lambda})}{e^{L/\lambda} (-1 + \frac{L}{\lambda}) + e^{-L/\lambda} (1 + \frac{L}{\lambda})}$$

$$B_4 = \frac{mh}{2} - B_3 = \frac{mh}{2} - \frac{\frac{mh}{2} e^{-L/\lambda} (1 + \frac{L}{\lambda})}{e^{L/\lambda} (-1 + \frac{L}{\lambda}) + e^{-L/\lambda} (1 + \frac{L}{\lambda})}$$

(3.1.11)

All of the coefficients are functions of known values, and most notably are a function of L/λ . Recalling our original equation, our resulting equation is,

$$v(x) = B_2x + B_3e^{x/\lambda} + B_4e^{-x/\lambda} , \quad (3.1.12)$$

where all the coefficients (B_2 , B_3 , and B_4) are now all solved for.

3.1.2 Evaluating the Service Condition

For the Service Condition, we have a very long bar where $L \rightarrow \infty$ (with respect to the wavelength λ). As, $L \rightarrow \infty$, we can see that the boundary conditions must still hold.

BC-1: B_3 and B_4 still may have finite values (possibly zero) as $L \rightarrow \infty$.

$$B_4 = \lambda^2 \frac{T}{EI} \frac{mh}{2} = \left(\frac{EI}{T}\right)^* \frac{T}{EI} \frac{mh}{2} = \frac{mh}{2}$$

BC-2: B_1 , B_3 and B_4 still may have finite values (possibly zero) as $L \rightarrow \infty$.

$$B_1 + B_4 = \frac{mh}{2}$$

BC-3 and BC-4: B_2 and B_3 must go to zero as $L \rightarrow \infty$, to prevent equation from blowing up.

Therefore, based on the terms expressed before, as $L \rightarrow \infty$,

$$B_2 \rightarrow 0$$

$$B_3 \rightarrow 0$$

and

$$B_4 \rightarrow \frac{mh}{2}$$

Now our general solution becomes:

$$v(x) = B_1 e^{-x/\lambda} = \frac{mh}{2} e^{-x/\lambda} \quad (3.1.13)$$

3.1.3 Analysis of the Ratio of Shear Force to Tensile Force

One general measure of the difference between the service conditions to the testing conditions is the ratio of the shear force to the tensile force. We know that the weld and heat affected zone (HAZ) is a rigid body, and rotates during the application of a tensile force, T . A diagram of the free body of the weld and HAZ is as follows before and after rotation is shown below in Figure 11, where M_g represents the moment near the grips.

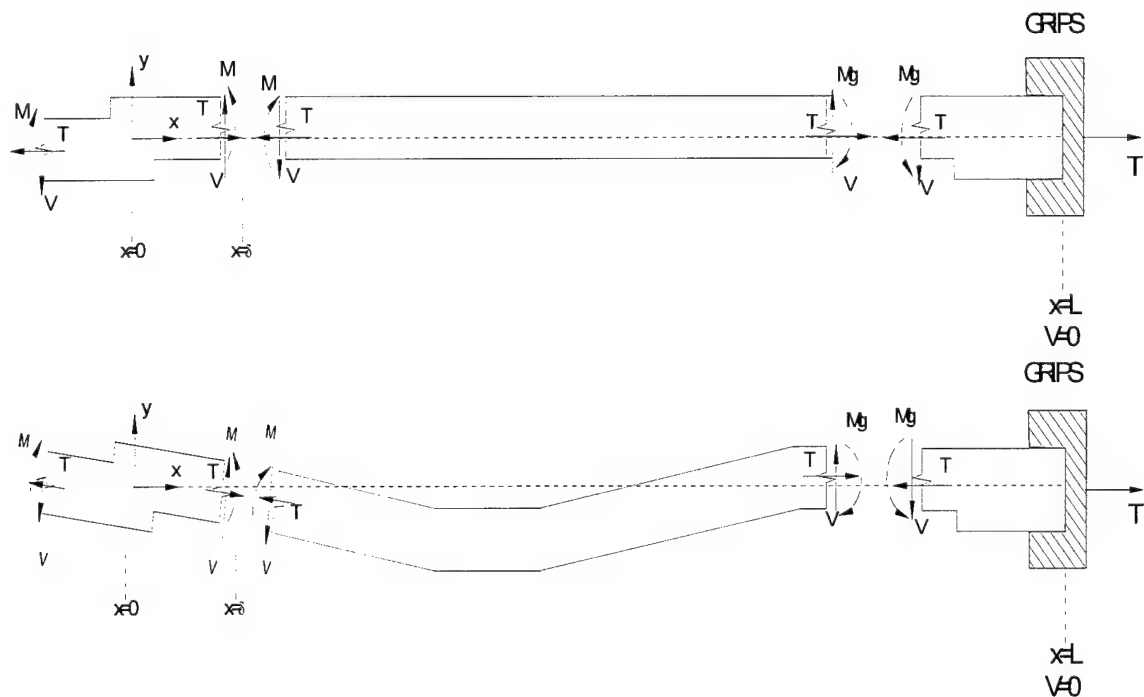


Figure 11. Before and after displacement applied to free body

As L goes to infinity, then V should go to zero. This maintains a constant M

We are concerned with the elastic portion that is present near the origin to the grips (see Figure 12).

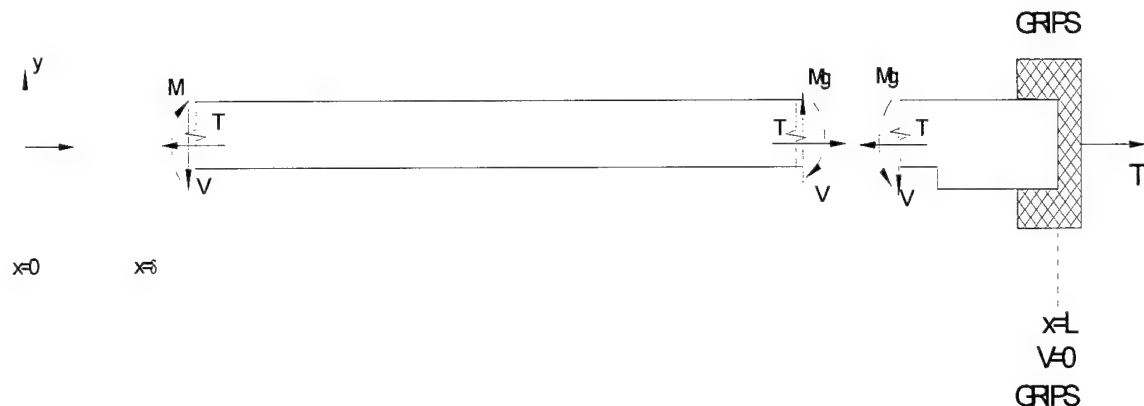


Figure 12. Free body diagram of infinite test case

T is a constant applied Force.

The shear force, V, varies a function of x, giving us $V(x)$.

We can evaluate the sum of the moments giving us,

$$\sum M = Mg + M = VL \quad (3.1.14)$$

which is composed of the bending moment near the origin,

$$M = T\left[\frac{mh}{2}\right] \quad (3.1.15)$$

and the bending moment near the grips,

$$Mg = EI \frac{d^2v(x)}{dx^2} = EI \frac{d^2}{dx^2} \left(\frac{mh}{2} e^{-L/\lambda}\right) = EI \frac{1}{\lambda^2} \frac{mh}{2} e^{-L/\lambda} \quad (3.1.16)$$

Using equation (3.1.2), we have,

$$Mg = EI \frac{1}{\lambda^2} \frac{mh}{2} e^{-L/\lambda} = EI \frac{T}{EI} \frac{mh}{2} e^{-L/\lambda} = T \frac{mh}{2} e^{-L/\lambda} \quad (3.1.17)$$

Therefore,

$$VL = Mg + M = T\left[\frac{mh}{2}\right] + T\left[\frac{mh}{2}\right]e^{-L/\lambda} = (1 + e^{-L/\lambda})T\left[\frac{mh}{2}\right] \quad (3.1.18)$$

Rearranging the equation we have:

$$\frac{V}{T} = (1 + e^{-L/\lambda})\left[\frac{mh}{2}\right]\frac{1}{L} \quad (3.1.19)$$

Using equation (3.1.2) and knowing that our λ is small compared to L , therefore the exponential term disappears, giving us:

$$\frac{V}{T} \approx \left[\frac{mh}{2}\right]\frac{1}{L} \quad (3.1.20)$$

Here, the variables (h , L , and T) are all constants. If we let L get larger, this would force V to get smaller. This checks out.

$$\frac{V}{T} \approx \frac{mh}{2}\frac{1}{L} \quad (3.1.21)$$

If we plug in our values for L , and h , we can get an idea of the relation between V and T . As before, m is the percent offset and is either 0%, 15%, or 30%.

$$\frac{V}{T} \approx \frac{mh}{2L} = \frac{(m)0.25in}{2(6.0in)} = \frac{m}{48} \quad (3.1.22)$$

Shear will therefore be an extremely small component, and may be ignored.

3.2 DESIGN OF SPECIMENS

3.2.1 Determining Specimen Measurements

A top-view drawing of our specimen as well as a side profile is seen in Figure 13.

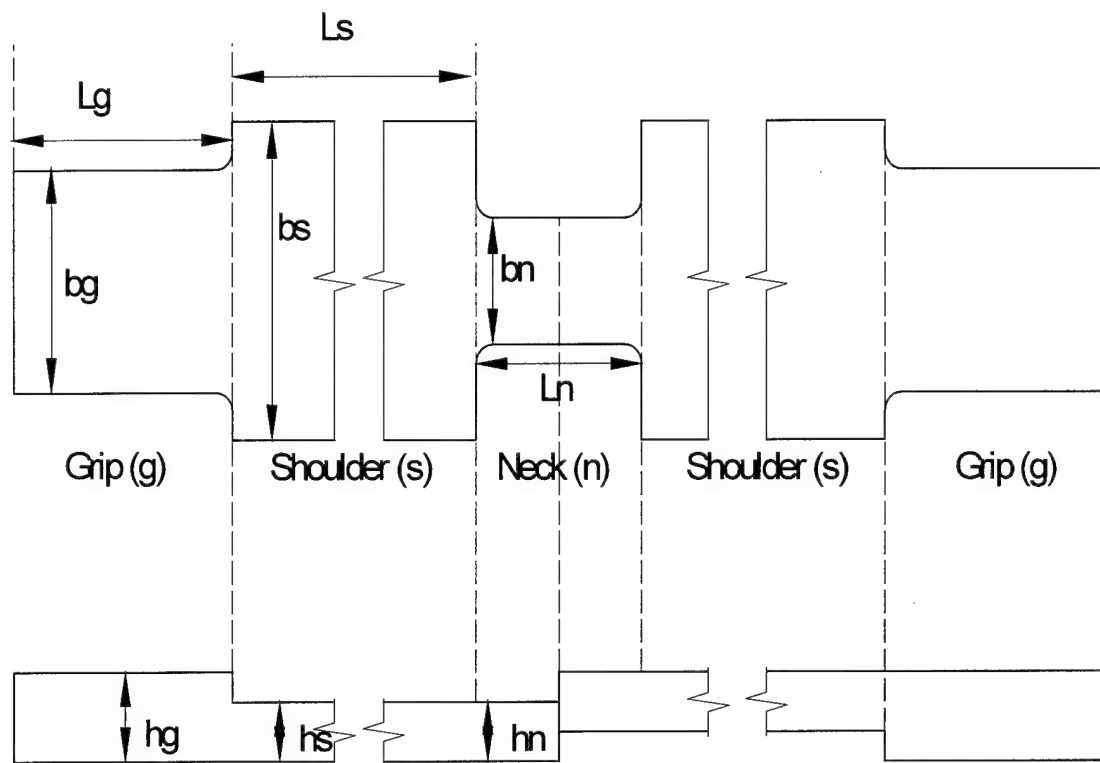


Figure 13. Top view drawing of specimen measurements

Nomenclature:

bn= width of neck Ln= length of neck hn = thickness of neck

bs= width of shoulder Ls= length of shoulder hs = thickness of shoulder

bg= width of grip Lg= length of grip hg = thickness of grip

YS= Yield Strength TS= Tensile Strength

Presumably there is no yielding in the center \rightarrow Plane Strain Condition.

The shoulders are built wide to prevent yielding in the shoulders. We want yielding to occur in the neck region.

The Grip region is designed so that it will not yield in grips under plane strain, while yielding occurs in the neck region (2/sqrt3*YS represents Plane Strain (PS)).

Strength in the grip region $P_g = (b_g)(h_g)(\frac{2}{\sqrt{3}}YS)$ (3.2.1)

Strength in the neck region $P_n = (b_n)(h_n)(\frac{2}{\sqrt{3}}TS)$ (3.2.2)

We want the neck region to fail in Plane Strain (PS), so the grip region should be “stronger” than neck region,

$$P_g > P_n \quad (3.2.3)$$

therefore, solving the equation as seen in Appendix F,

$$b_g > \left(\frac{2}{\sqrt{3}} \frac{TS}{YS} \right) (b_n) \quad (3.2.4)$$

We want the shoulder region to not yield in uniaxial stress while the neck region is yielding in plane strain, so the shoulder region should be “stronger” than the neck region,

Strength in the shoulder region $P_s = (b_s)(h_s)(YS)$, (3.2.5)

$$P_s > P_n \quad (3.2.6)$$

therefore, solving the equation as seen in Appendix F,

$$b_g > \left(\frac{TS}{YS} \frac{h_n}{h_g} \right) (b_n) \quad (3.2.7)$$

This will ensure yielding in the neck, and to prevent yielding in the shoulders

APPLYING RESULTS FOR SPECIMEN CROSS SECTION

The grips have size limitations where: $(b_g)_{\max} = 50mm = 1.968in$

It is important to have the largest neck region as possible, as this allows us to have increased thickness in the neck and still maintain the plane strain condition. Solving equations for b_n , using the given value for b_g in equation, and plugging in values for both tensile and yield stresses, and the heights we get the resulting widths. These widths are seen in a data table for each type of steel being tested (EH-36 and AL6XN) for each of the three different offset conditions (0%, 15%, and 30%). Also, a simplification can be made based on the fact that the grip region is sized such that $h_g = h_n + mh$, where $mh = \text{offset}, (m = \% \text{ offset})$ and $h = h_n = h_s$. This gives us $h_g = h_n + mh = h_n + mh_n = (1 + m)h_n$, and the final useful result is $\frac{h_n}{h_g} = \frac{1}{1 + m}$. For our three different conditions, offsets of (0%, 15%, and 30%) give corresponding $\frac{h_n}{h_g}$ values of (1.0, 0.8696, 0.7692) respectively.

The Tensile and Yield Stresses for the two steels are:

	EH36	AL6XN
Tensile Strength	78,000 psi	112,000 psi
Yield Strength	~56,000 psi	~53,000 psi

Table 3. Material properties of EH 36 and AL6XN

For EH-36 Mild Steel:

	b_g	b_s	b_n
0% offset	1.96 in	2.30 in	1.40 in
15% offset	1.96 in	2.60 in	1.60 in
30% offset	1.96 in	3.00 in	1.80 in

Table 4. Measurements for EH 36 at varying offsets

For AL6XN Stainless Steel:

	b_g	b_s	b_n
0% offset	1.96 in	2.30 in	0.92 in
15% offset	1.96 in	2.60 in	1.05 in
30% offset	1.96 in	3.00 in	1.20 in

Table 5. Measurements for AL6XN at varying offsets

In summary, assuming we want to make the largest specimen we can, our limiting factor is the size of the grips (in our case 50 mm = 1.96 in).

3.3 TESTING OF SPECIMENS

A MTS Model RF/200 floor standing testing machine was used to test the various specimens. The specimen plates were placed vertically into the opposing grips. They were fitted with an extensometer in the neck region around the weld. A constant displacement rate will be applied to the grips. The applied force on the load cell and the extensions were measured and recorded using computers.

The various specimens consisted of two different types of steel: a medium strength steel, EH-36, and a new stainless steel, AL6XN. Each type of steel had specimens with three different offsets: 0%, 15%, and 30%.

CHAPTER 4 RESULTS

4.1 EXPERIMENT CRITERION

4.1.1 Specimen Fabrication

A total of 18 specimens were tested consisting of 9 each of EH-36 and AL6XN, respectively. For each of the three offset conditions (0%, 15%, 30%), a total of three specimens were created thereby giving the previously stated 9 specimens of each material. Based on the tolerances that exist in manufacturing the specimens, there is a slight variance about each of the presupposed offsets. For the 15% case of the EH-36, the actual offsets ended up being (16%, 15% and 14.5%). Similar offset variance was noted for the remaining specimens. This phenomenon was anticipated and will help give realistic continuity to the acquired data and results.

The EH-36 was machined in the Central Machining Plant at MIT into rectangular plates and then welded at Bath Iron Works. The AL6XN was both machined and welded at Metro Machines in Philadelphia, PA. The final specimens were water-jetted out at MIT.

4.1.2 Testing of the design specimens

Figure 14 shows a sample of an EH-36 specimen with a 30% offset. As described previously, this specimen was placed in the MTS Model RF/200 floor-standing testing machine for analysis. It was fitted with an extensometer around

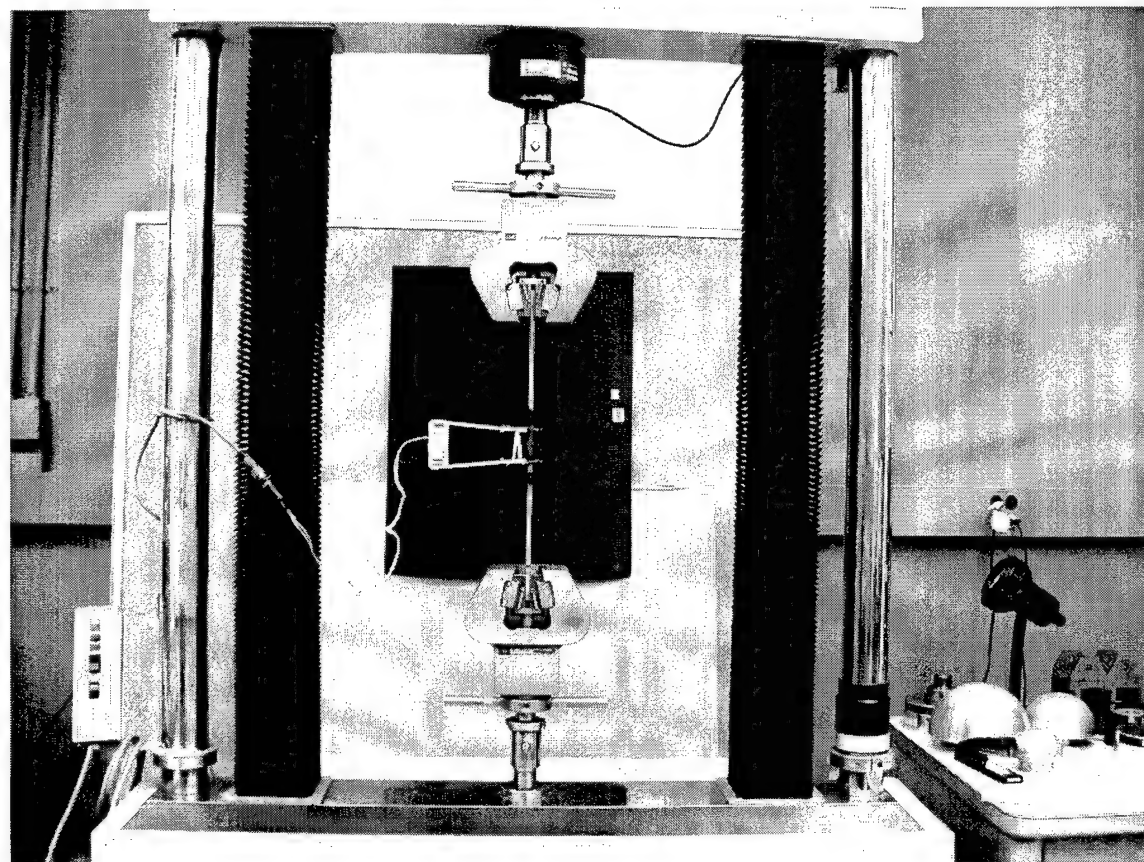


Figure 14. MTS testing machine with specimen in grips

the weld region. A steady velocity was then applied at a constant rate of 0.00167 in/sec (or 0.1 in/min). Shortly after the maximum loading was observed, and the loading started to decrease as the specimen began necking, the experiment was stopped. A schematic of each of the offset cases is shown in Appendix G.

4.2 EXPERIMENTAL RESULTS

4.2.1 EH-36 Experimental Results

The EH 36 specimens produced relatively uniform data for the force/area vs. gauge strain graphs shown in Appendix H. The results are tabulated below in Table 6.

Property	0% Offset	15 % Offset	30% Offset
Force/Area at Point of Yield	54 kpsi	55 kpsi	55 kpsi
Force/Area at Point of Necking	80 kpsi	81 kpsi	80 kpsi
Gauge Strain to Yield	.016	.015	.015
Gauge Strain to Necking	.11	.10	.11

Table 6. Summary of test results of EH 36 specimens

4.2.2 AL6XN Experimental Results

The AL6XN specimens produced relatively uniform data for the force/area vs. gauge strain graphs shown in Appendix H. The results are tabulated below in Table 7.

Property	0% Offset	15 % Offset	30% Offset
Force/Area at Point of Yield	54 kpsi	55 kpsi	53 kpsi
Force/Area at Point of Necking	115 kpsi	116 kpsi	108 kpsi
Gauge Strain to Yield	.015	.014	.015
Gauge Strain to Necking	.15	.14	.16

Table 7. Summary of test results for AL6XN

4.2.3 Analysis of Experimental Results

The EH-36 specimens exhibited typical mild strength steel properties. The applied force/unit area vs. gauge strain curves for all nine EH-36 specimens are shown in Appendix H. A description of the data collection and processing is recorded in Appendix B. Similarly, the AL6XN specimens exhibited typical high strength stainless steel properties. The applied force/unit area vs. gauge strain curves for all nine AL6XN specimens are shown in Appendix I.

As the displacement was increasing and the material began yielding the weld/HAZ region rotated, as expected. After the EH 36 rotated, no further deformation in the material near the weld occurred. This was possibly the effect of strain hardening occurring as a result of the rotation. Further analysis using FEA, with the new assumption of strain hardening was done in both the 2D and 3D cases.

The new 2D FEA results shown in Figures 15 and 16 show the strain hardening resisting further shear banding near the weld, and causing the material to neck elsewhere. This was consistent with the results of the experiment.

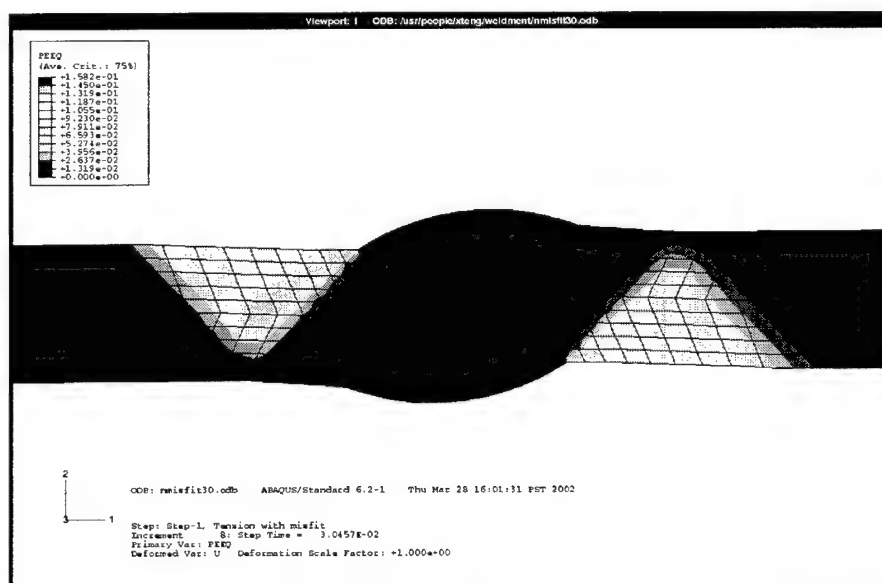


Figure 15. 2D FEA analysis of EH36 without Strain hardening (30% offset)

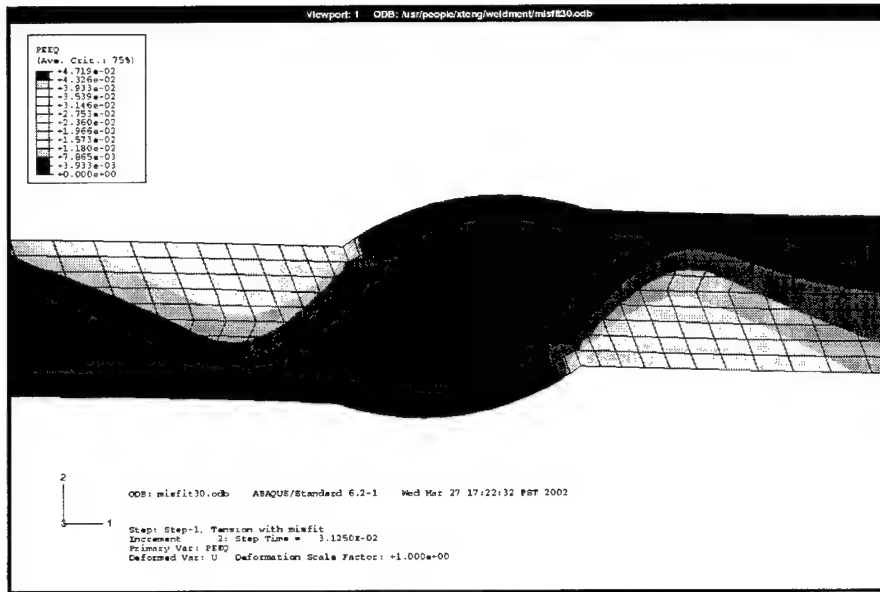


Figure 16. 2D FEA analysis of EH36 with Strain hardening (30% offset)

A 3D FEA model was also created with strain hardening accounted for. The results with this model are shown in Figure 17. The failure mode evident in this FEA model is nearly the same as that experienced in all of the experiments.

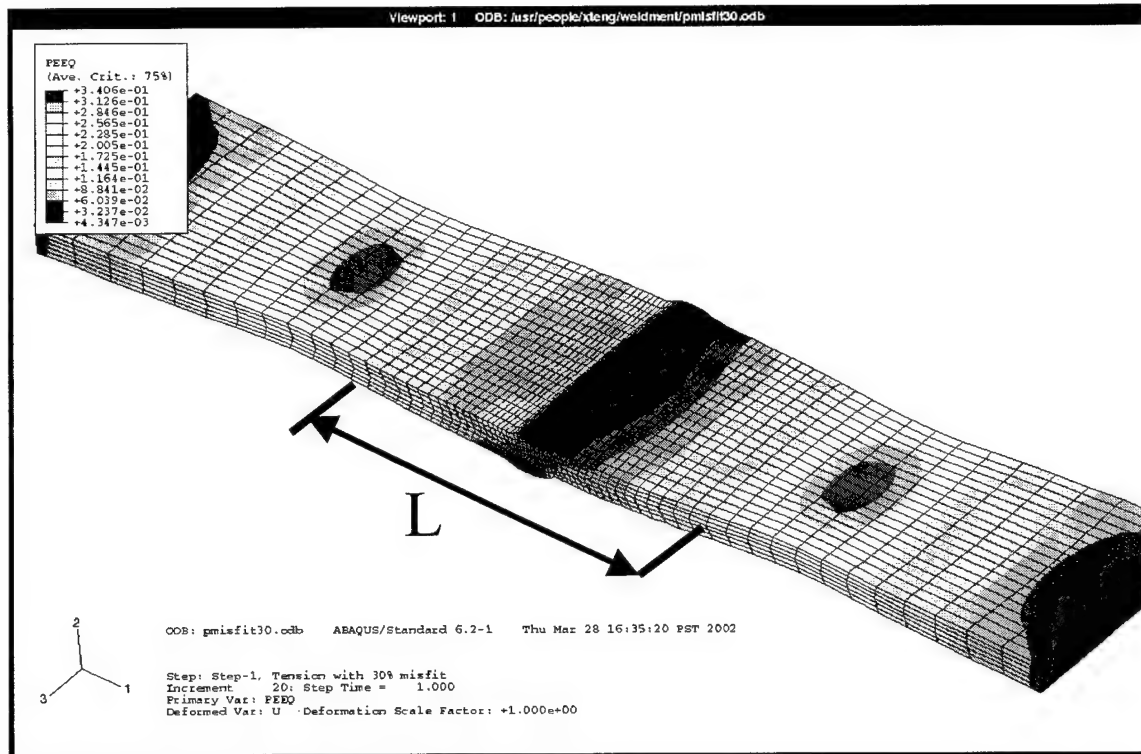


Figure 17. 3D FEA Model of EH36 with Strain Hardening (30% offset). The gauge length is denoted by L.

A comparison of the results from SLFM and FEA, comparing rotation angle versus normalized elongation is shown in Figure 18. The dashed lines shown represent the boundaries of the spread of the experimental results that were observed during the testing. It is not certain as to the reason for the sharp rise in FEA that occurs around a normalized elongation of 0.01, although it does taper off due to strain hardening as expected.

The rotation of the offset welds was measured using a thin metal wire and recorded using digital photographs. The metal wire was attached to the weld using an epoxy. During the experiment, digital photographs were taken at 30-

second intervals. Rotation was then calculated by comparing the wire's orientation in the sequential pictures to the initial orientation.

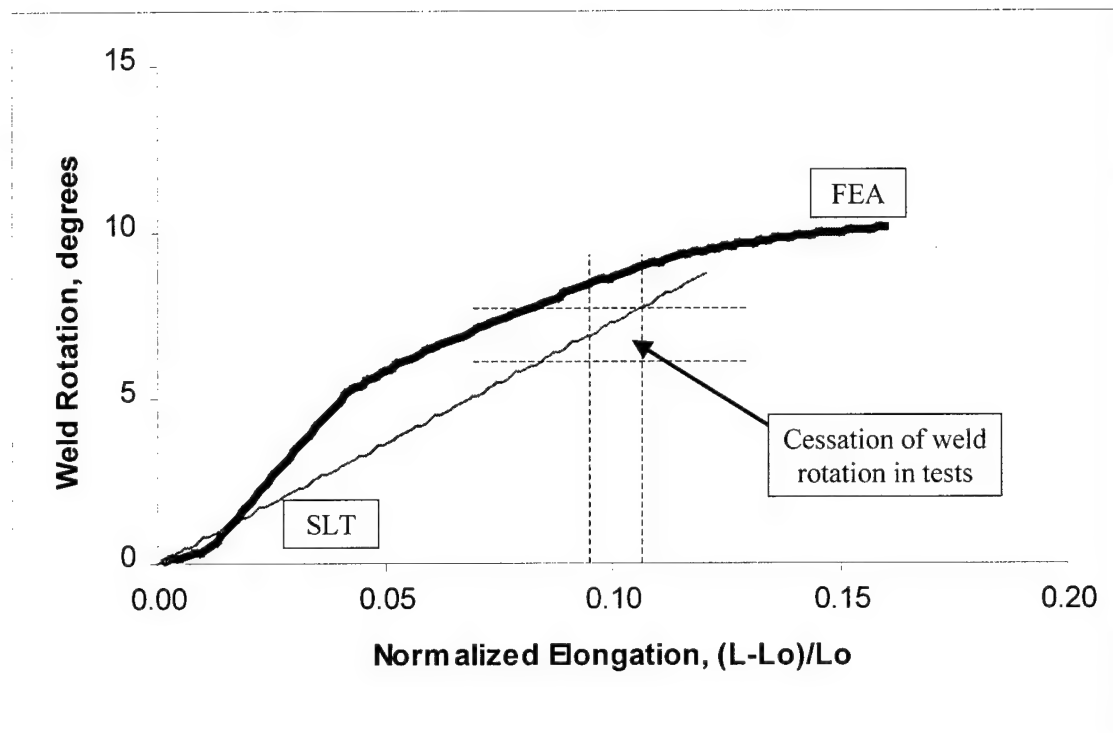


Figure 18. Weld rotation versus Normalized Elongation of overmatched EH36 (30% offset). Cessation of weld rotation occurred and is represented by the dashed lines.

A comparison of the results from SLT, FEA, and experiments regarding the applied load per area versus normalized elongation is shown in Figure 19. The approximate area where the applied forces became aligned and the weld stopped rotating is annotated as "Aligned". The approximate area where the material became rigid is annotated as "Rigid".

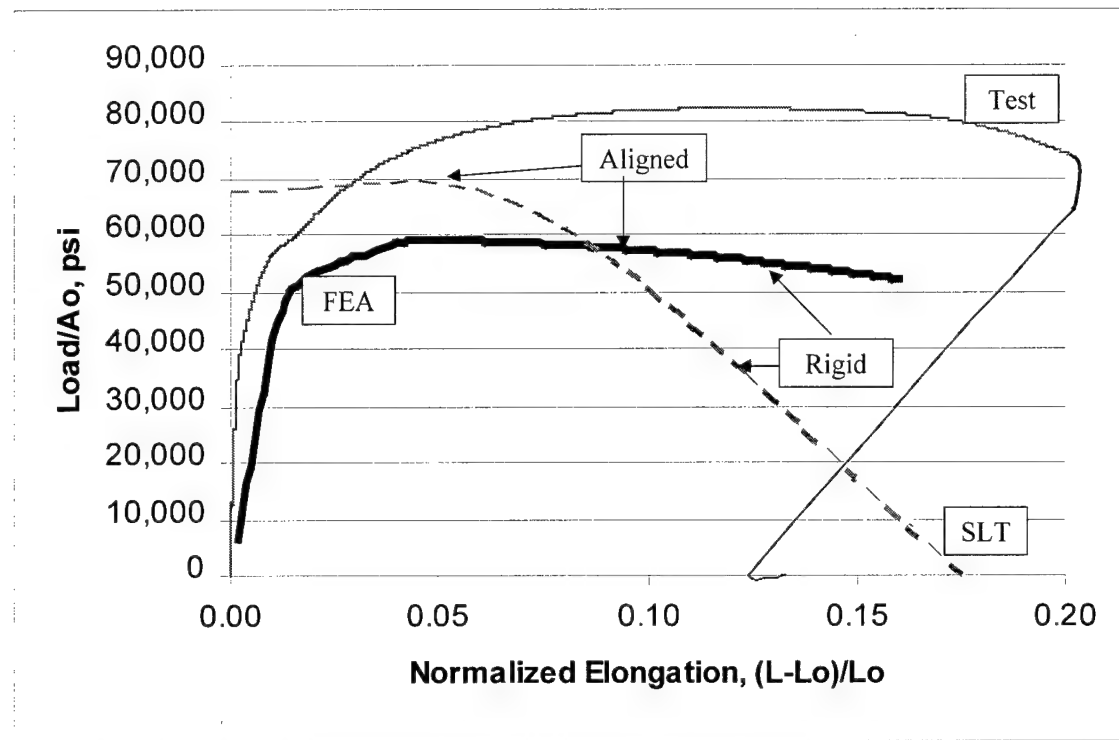


Figure 19. Load per Area vs. Normalized Elongation of overmatched EH-36 with strain hardening. (30% offset).

It is noted that there was thinning of the specimens near the weld. This was more pronounced for the evenmatched AL6XN than for the overmatched EH-36. Further thinning was arrested by the strain hardening that occurred during the weld rotation. Analyzing the 30% offset cases, from an original thickness of 0.25 inches, the AL6XN had thinning near the weld to 0.23 inches with increased localized thinning of an additional 0.0177 inches. The EH-36, with an original thickness of 0.25 inches, thinned down to 0.24 inches, with an increased localized thinning of an additional 0.0059 inches.

The EH-36 had 4% thinning near the weld with an additional localized thinning of 2.3%. The AL6XN had 8% thinning near the weld with an additional localized thinning of 7.1%

CHAPTER 5 DISCUSSION AND CONCLUSIONS

5.1 DISCUSSION

As expected the welds in the offset cases rotated in order to remove the offset and the resultant moment. However, this rotation caused strain hardening and thinning to occur in the base metal next to the weld region. This strain hardening resisted further shear bands from developing, and causing failure to occur away from the weld. The strain hardening dominated the thinning and resulted in failure away from the weld. The strain hardening limits loss of strength to at most 3% for welds with offsets up to 30%. Only tensile loads were studied.

Slip Line Theory (SLT) was useful in giving closed form expressions for the deformation and rigid body motions near an offset weld and Finite Element Analysis (FEA) included more realistic geometry and strain hardening. The

rotation of the offset weld was on the order of 0.25 degrees per % of offset. FEA suggested some aspects of the field, which in turn guided mesh refinement. The FEA allowed the introduction of strain hardening. This synergism improves the prediction of the experimental results.

In two experiments, one each of EH-36 and AL6XN, the extension was continued to complete separation. The failure occurred as necking in the parent plating away from the weld. It is not clear whether or not that this necking occurs under the plain strain condition in the weld direction that is typical of service. These failures were confirmed by the 3D-case simulated using FEA.

5.2 RECOMMENDATIONS FOR FURTHER STUDY

There is material available to create specimens for further testing. Enough EH-36 exists to create at least 8 more specimens, and enough AL6XN for 3 more specimens. Based on the experimental result, further analysis using FEA and SLT can also be done to better understand and approximate the failure of ship hull plating with varying misfit and mismatch welds.

More attention should be paid to the 2D FEA study as its boundary conditions more closely represent the actual boundary conditions of the ship hull plating. Also, more in depth SLT and FEA analysis of crack growth and sliding after the initial weld rotation removes the offset should be performed. 2D FEA should be used to predict effects of mismatch and misfit with lower Tensile/Yield ratios.

Lastly, it would prove useful to perform FEA studies on more evenmatched and undermatched welds with the associated weld geometries to compare with these experiments.

5.3 CONCLUSIONS

For EH-36, with overmatched welds, there is no apparent reduction in strength for weld offsets up to 30%. This should apply to other overmatched welded steels with similar Tensile/Yield ratios (~1.5).

For AL6XN, with evenmatched welds, there is no apparent reduction in strength for weld offsets up to 15%, and there is at most a 3% reduction in strength for weld offsets of up to 30%. This slight reduction in maximum applied force/area can be attributed to variance in the experimental process. This should apply to other evenmatched welded steels with similar Tensile/Yield ratios (~2.0).

For the overmatched EH-36 welded plating, there is no apparent benefit of increased precision manufacturing with regards to welding with reduced misfit of ship hull plating based on the current standards [8]. For the evenmatched AL6XN welded plating, it is inconclusive without further study whether any benefit could be gained from precision manufacturing.

CHAPTER 6 REFERENCES

- [1] McClintock, Frank A., Parks, David M., and Holmes, John W. (1984) "Drop in K_I due to load shift in single-edge notch tests with compliant drawbars", *Engineering Fracture Mechanics*, Vol. 20, No.1, pp. 159-167.
- [2] Masubuchi, Koichi and R.G. Morris (2000) "A Welding Research and Engineering Festschrift", MIT Press, pp. 275-312
- [3] Popov, Egor P. (1968) "Introduction to Mechanics of Solids", Prentice-Hall.
- [4] Shames, Irving H. (1989) "Introduction to Solid Mechanics", Prentice-Hall.
- [5] Konkol, Paul J., Kenneth M. Sabo, Gerard P. Mercier, Keith R. Miller, Frederick D. Arnold (2000) "Evaluation of Forming, Flame Bending, and Welding of ABS Grade EH-36 Steel Plates", National Center for Excellence in Metalworking Technology, Limited distribution.
- [6] Teng, Xiaoqing (2001) "Numerical Simulation of Effects of Mismatch and Misfit on Response of Butt-welded Plates", MIT Impact and Crashworthiness Laboratory, Report #52.
- [7] Weaver, M. Cameron (2001), Thesis, "Ship Hull Plating Weld Misalignment Effects when Subjected to Tension", MIT Impact and Crashworthiness Laboratory, Report #6
- [8] MIL-STD-1689A(SH).
- [9] Forrest, David and Dean Brown (2002). Welding information provided at and by Bath Iron Works.
- [10] Chakrabarty, J. (1987), "Theory of Plasticity", McGraw-Hill

APPENDIX A SPECIMEN CALCULATIONS

Specimen dimension calculations for flat specimen:

Given:

Tensile Strength, TS of EH-36

$$TS = 78 \text{ kpsi}$$

MTS test machine rating of 200 kN (44961 lbs).

Design to use only one-half of MTS machine rating, F.

$$TS = \frac{P}{A}$$

$$A = bh$$

where A is the area, b is the specimen width, and b is the specimen thickness.

Solving for P,

$$P = A(TS) = (b \text{ in})(0.25 \text{ in})(TS \text{ lbs/in}^2)$$

$$\frac{P}{F} = \frac{P \text{ lbs}}{44961 \text{ lbs}}$$

A table for each of the specimens is shown.

For EH-36:

	b (in)	h (in)	Area (in ²)	TS (lbs/in ²)	P (lbs)	F (lbs)	P/F ratio
0% offset	1.40	0.25	0.35	78,000	27,300	44,961	0.6072
15% offset	1.60	0.25	0.40	78,000	31,200	44,961	0.6939
30% offset	1.80	0.25	0.45	78,000	35,100	44,961	0.7807

For AL6XN:

	b (in)	h (in)	Area (in ²)	TS (lbs/in ²)	P (lbs)	F (lbs)	P/F ratio
0% offset	0.92	0.25	0.23	112,000	25,760	44,961	0.5729
15% offset	1.05	0.25	0.26	112,000	29,400	44,961	0.6539
30% offset	1.20	0.25	0.30	112,000	33,600	44,961	0.7473

Thus the force, P, required to break the specimen is approximately between one-half and three-quarters of the capability of the machine.

APPENDIX B EH 36 PLATE SPECIMEN TEST DATA

Calibration Data:

Load in lbf

Extension in inches

Gage length = 2.0 in

Area = width * thickness

thickness = 0.25 in for all cases

width = 1.8 in for 30% offset case

width = 1.6 in for 15% offset case

width = 1.4 in for 0% offset case

Calculations:

$$\text{Engineering Stress} = \frac{\text{Load(lbf)}}{\text{Area}(in^2)}$$

$$\text{Gauge Strain (in/in)} = \frac{\text{Extension (in)}}{\text{Gauge Length (in)}}$$

APPENDIX C AL6XN PLATE SPECIMEN TEST DATA

Calibration Data:

Load in lbf

Extension in inches

Gage length = 2.0 in

Area = width * thickness

thickness = 0.25 in for all cases

width = 1.2 in for 30% offset case

width = 1.05 in for 15% offset case

width = 0.92 in for 0% offset case

Calculations:

$$\text{Engineering Stress} = \frac{\text{Load(lbf)}}{\text{Area}(in^2)}$$

$$\text{Gauge Strain (in/in)} = \frac{\text{Extension (in)}}{\text{Gauge Length (in)}}$$

APPENDIX D BOUNDARY CONDITION CALCULATIONS

Evaluating [BC-1],

$$EI \frac{d^2v(x=0)}{dx^2} = T \frac{mh}{2}$$

which can be expressed as,

$$\frac{d^2v(x=0)}{dx^2} = \frac{T}{EI} \frac{mh}{2}$$

and this can be expanded using equation to give us ,

$$\frac{d^2v(x=0)}{dx^2} = \left(\frac{1}{\lambda}\right)^2 B_3 e^{(0)/\lambda} + \left(\frac{-1}{\lambda}\right)^2 B_4 e^{-(0)/\lambda} = \left(\frac{1}{\lambda}\right)^2 B_3 e^0 + \left(\frac{-1}{\lambda}\right)^2 B_4 e^0 = \left(\frac{1}{\lambda}\right)^2 B_3 + \left(\frac{-1}{\lambda}\right)^2 B_4$$

$$\frac{d^2v(x=0)}{dx^2} = \frac{T}{EI} \frac{mh}{2}$$

$$\left(\frac{1}{\lambda}\right)^2 B_3 + \left(\frac{-1}{\lambda}\right)^2 B_4 = \left(\frac{1}{\lambda}\right)^2 [B_3 + B_4] = \frac{T}{EI} \frac{mh}{2}$$

$$B_3 + B_4 = \lambda^2 \frac{T}{EI} \frac{mh}{2} = \frac{EI}{T} \frac{T}{EI} \frac{mh}{2} = \frac{mh}{2}$$

Evaluating [BC-2],

$$v(x=0) = v_{\max} = \frac{mh}{2},$$

substituting in equation, gives,

$$v(x=0) = B_1 + B_2(x=0) + B_3 e^{(x=0)/\lambda} + B_4 e^{-(x=0)/\lambda} = B_1 + B_3 + B_4 = U_{\max} = \frac{mh}{2}$$

$$B_1 + B_3 + B_4 = \frac{mh}{2}$$

Evaluating [BC-3],

$$v(x = L) = 0$$

substituting in equation, we get,

$$v(x = L) = B_1 + B_2(L) + B_3 e^{(L)/\lambda} + B_4 e^{(L)/\lambda} = 0$$

$$B_1 + B_2 L + B_3 e^{L/\lambda} + B_4 e^{-L/\lambda} = 0$$

Evaluating [BC-4],

$$\frac{dv(x = L)}{dx} = 0$$

substituting in equation , we get,

$$\frac{dv(x = L)}{dx} = B_2 + \left(\frac{1}{\lambda}\right) B_3 e^{(L)/\lambda} + \left(\frac{-1}{\lambda}\right) B_4 e^{-(L)/\lambda} = 0$$

$$B_2 + \frac{1}{\lambda} B_3 e^{L/\lambda} - \frac{1}{\lambda} B_4 e^{-L/\lambda} = 0$$

We now have 4 equations with 4 unknowns (B₁, B₂, B₃, and B4):

$$B_3 + B_4 = \frac{mh}{2}$$

$$B_1 + B_3 + B_4 = \frac{mh}{2}$$

$$B_1 + B_2 L + B_3 e^{L/\lambda} + B_4 e^{-L/\lambda} = 0$$

$$B_2 + \frac{1}{\lambda} B_3 e^{L/\lambda} - \frac{1}{\lambda} B_4 e^{-L/\lambda} = 0$$

T, E, I, L, λ , and h are all known or measurable quantities.

APPENDIX E SERVICE CONDITION EVALUATION CONDITION

For the Service Condition, we have a very long bar where $L \rightarrow \infty$ (a very long bar with respect to the wavelength λ). As, $L \rightarrow \infty$, we can see that the boundary conditions must still hold.

BC-1: B_3 and B_4 still may have finite values (possibly zero) as $L \rightarrow \infty$.

$$B_4 = \lambda^2 \frac{T}{EI} \frac{mh}{2} = \left(\frac{EI}{T}\right)^* \frac{T}{EI} \frac{mh}{2} = \frac{mh}{2}$$

BC-2: B_1 , B_3 and B_4 still may have finite values (possibly zero) as $L \rightarrow \infty$.

$$B_1 + B_4 = \frac{mh}{2}$$

BC-3 and BC-4: B_2 and B_3 must go to zero as $L \rightarrow \infty$, to prevent equation from "blowing up".

As $L \rightarrow \infty$,

terms with $e^{-L/\lambda} \rightarrow 0$

terms with $e^{L/\lambda} \rightarrow \infty$

terms with $Le^{-L/\lambda} \rightarrow 0$ (by L'Hopital's rule)

terms with $Le^{L/\lambda} \rightarrow \infty$

Therefore, based on the terms expressed before,

As $L \rightarrow \infty$,

$$B_1 = 0$$

$$B_2 \rightarrow 0$$

$$B_3 \rightarrow 0$$

$$B4 \rightarrow \frac{mh}{2}$$

Now our general solution becomes:

$$v(x) = B_1 + B_2x + B_3e^{x/\lambda} + B_4e^{-x/\lambda} = B_4e^{-x/\lambda} = \frac{mh}{2}e^{-x/\lambda}$$

APPENDIX F DETERMINING SPECIMENT MEASUREMENTS

1. Shoulder region to be “stronger” than Neck region

$$P_s > P_n$$

$$(b_s)(h_s)(YS) > (b_n)(h_n)(\frac{2}{\sqrt{3}} TS)$$

but,

$$h_s = h_n$$

so,

$$(b_s)(YS) > (b_n)(\frac{2}{\sqrt{3}} TS)$$

$$\frac{b_s}{b_n} > \frac{2}{\sqrt{3}} \frac{TS}{YS}$$

therefore,

$$b_s > \left(\frac{2}{\sqrt{3}} \frac{TS}{YS} \right) (b_n)$$

2. Grip region to be “stronger” than Neck region

$$P_g > P_n$$

$$(b_g)(h_g)(\frac{2}{\sqrt{3}} YS) > (b_n)(h_n)(\frac{2}{\sqrt{3}} TS)$$

$$(b_g)(h_g)(YS) > (b_n)(h_n)(TS)$$

$$\frac{b_g}{b_n} > \frac{TS}{YS} \frac{h_n}{h_g}$$

therefore,

$$b_g > \left(\frac{TS}{YS} \frac{h_n}{h_g} \right) (b_n)$$

APPLYING RESULTS FOR SPECIMEN CROSS SECTION

For EH-36 Steel

$$TS := 78000 \text{ psi} \quad YS := 56000 \text{ psi}$$

$$bg := 1.96 \text{ in}$$

$$\text{Case 1: } m := 0.000$$

$$bn := \left(\frac{YS}{TS} \cdot \frac{1+m}{1} \right) \cdot bg \quad bn = \blacksquare \text{ in} \quad \text{Let } bn := 1.40 \text{ in}$$

$$bs := \left(\frac{2}{\sqrt{3}} \cdot \frac{TS}{YS} \right) \cdot bn \quad bs = \blacksquare \text{ in} \quad \text{Let } bs := 2.30 \text{ in}$$

$$\text{Case 2: } m := 0.150$$

$$bn := \left(\frac{YS}{TS} \cdot \frac{1+m}{1} \right) \cdot bg \quad bn = \blacksquare \text{ in} \quad \text{Let } bn := 1.60 \text{ in}$$

$$bs := \left(\frac{2}{\sqrt{3}} \cdot \frac{TS}{YS} \right) \cdot bn \quad bs = \blacksquare \text{ in} \quad \text{Let } bs := 2.60 \text{ in}$$

$$\text{Case 3: } m := 0.300$$

$$bn := \left(\frac{YS}{TS} \cdot \frac{1+m}{1} \right) \cdot bg \quad bn = \blacksquare \text{ in} \quad \text{Let } bn := 1.80 \text{ in}$$

$$bs := \left(\frac{2}{\sqrt{3}} \cdot \frac{TS}{YS} \right) \cdot bn \quad bs = \blacksquare \text{ in} \quad \text{Let } bs := 3.00 \text{ in}$$

	b_g	b_s	b_n
0% offset	1.96 in	2.30 in	1.40 in
15% offset	1.96 in	2.60 in	1.60 in
30% offset	1.96 in	3.00 in	1.80 in

For AL6XN Stainless Steel

$$TS := 112000 \text{ psi} \quad YS := 53000 \text{ psi}$$

$$bg := 1.96 \text{ in}$$

Case 1: $m := 0.000$

$$bn := \left(\frac{YS}{TS} \cdot \frac{1+m}{1} \right) \cdot bg \quad bn = \blacksquare \text{ in} \quad \text{Let } bn := 0.92 \text{ in}$$

$$bs := \left(\frac{2}{\sqrt{3}} \cdot \frac{TS}{YS} \right) \cdot bn \quad bs = \blacksquare \text{ in} \quad \text{Let } bs := 2.30 \text{ in}$$

Case 2: $m := 0.150$

$$bn := \left(\frac{YS}{TS} \cdot \frac{1+m}{1} \right) \cdot bg \quad bn = \blacksquare \text{ in} \quad \text{Let } bn := 1.05 \text{ in}$$

$$bs := \left(\frac{2}{\sqrt{3}} \cdot \frac{TS}{YS} \right) \cdot bn \quad bs = \blacksquare \text{ in} \quad \text{Let } bs := 2.60 \text{ in}$$

Case 3: $m := 0.300$

$$bn := \left(\frac{YS}{TS} \cdot \frac{1+m}{1} \right) \cdot bg \quad bn = \blacksquare \text{ in} \quad \text{Let } bn := 1.20 \text{ in}$$

$$bs := \left(\frac{2}{\sqrt{3}} \cdot \frac{TS}{YS} \right) \cdot bn \quad bs = \blacksquare \text{ in} \quad \text{Let } bs := 3.00 \text{ in}$$

	b_g	b_s	b_n
0% offset	1.96 in	2.30 in	0.92 in
15% offset	1.96 in	2.60 in	1.05 in
30% offset	1.96 in	3.00 in	1.20 in

APPENDIX G DESIGN SCHEMATICS OF TEST SPECIMENS

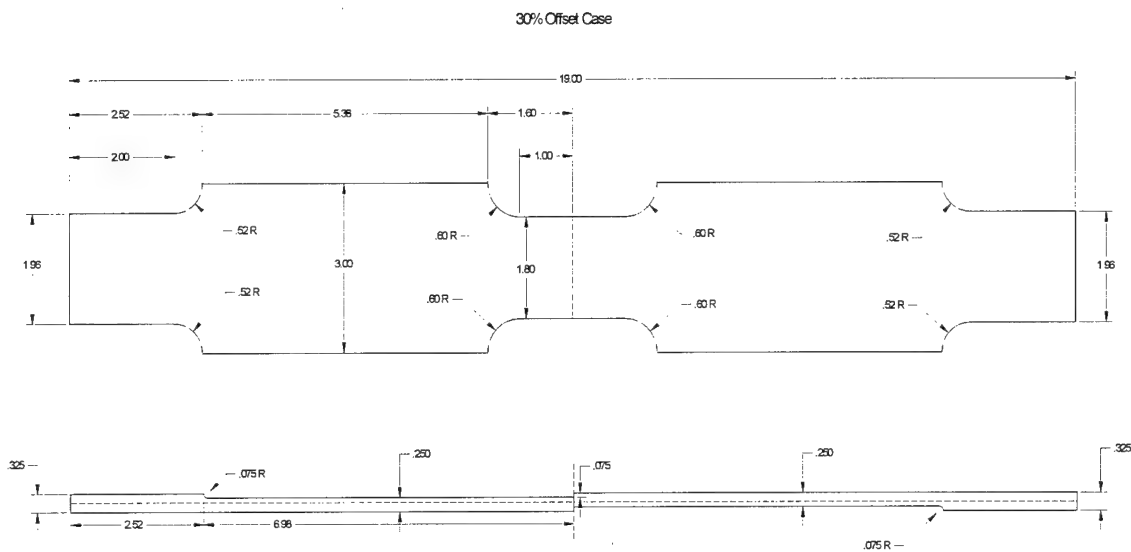


Figure 20. 30% offset case

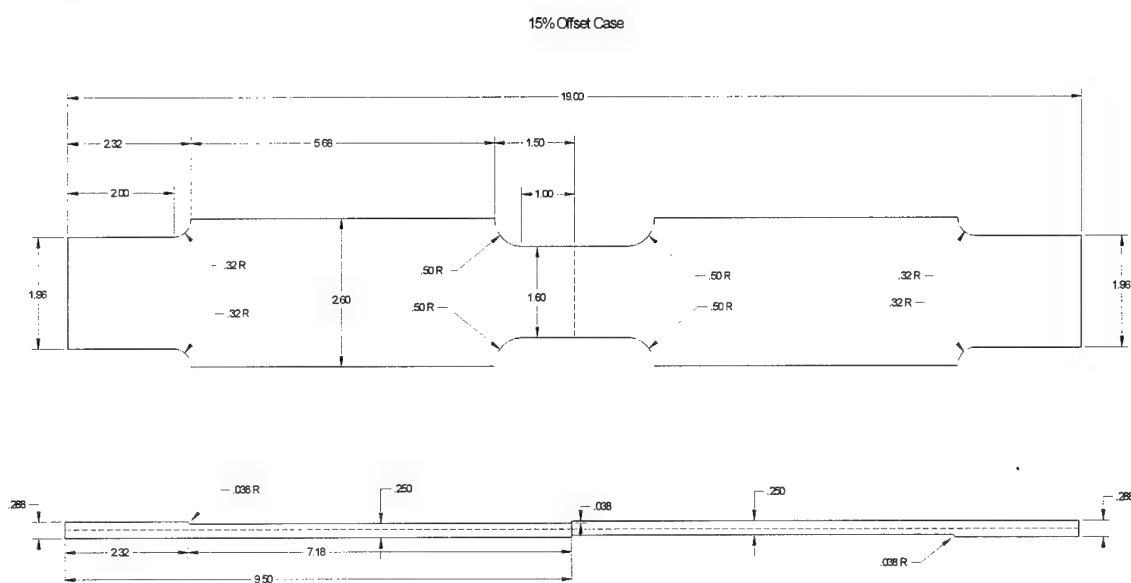


Figure 21. 15% offset case

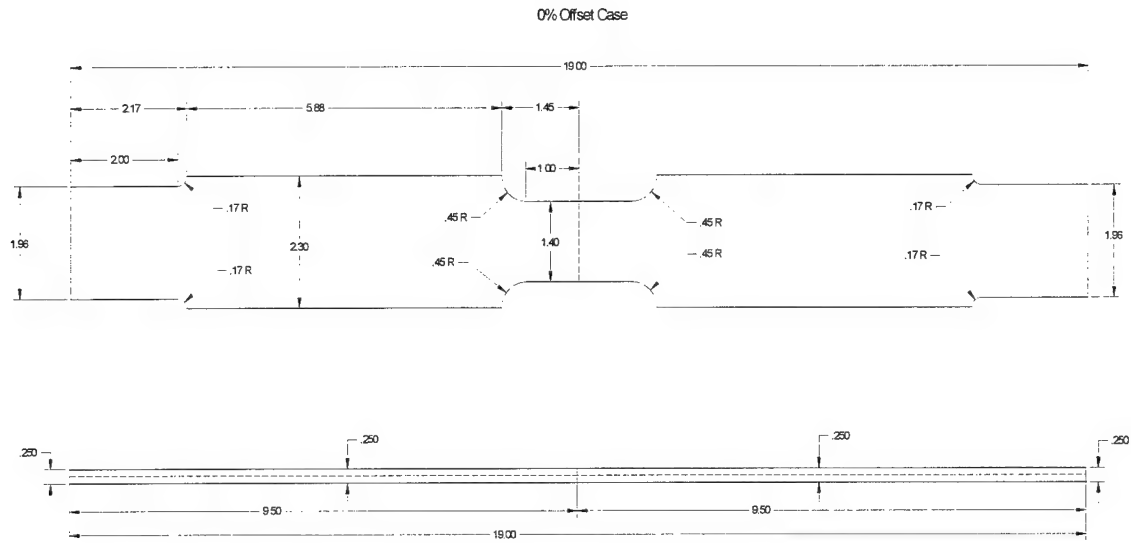
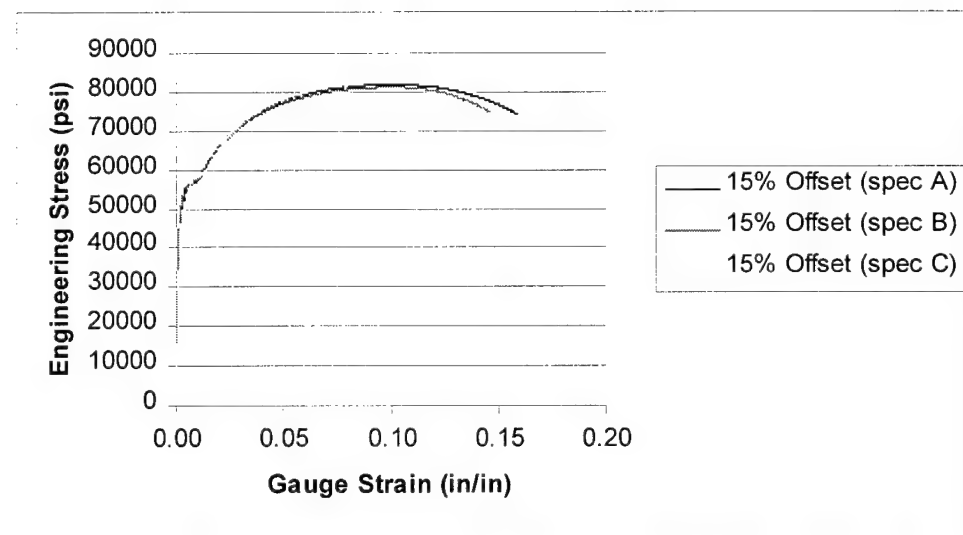
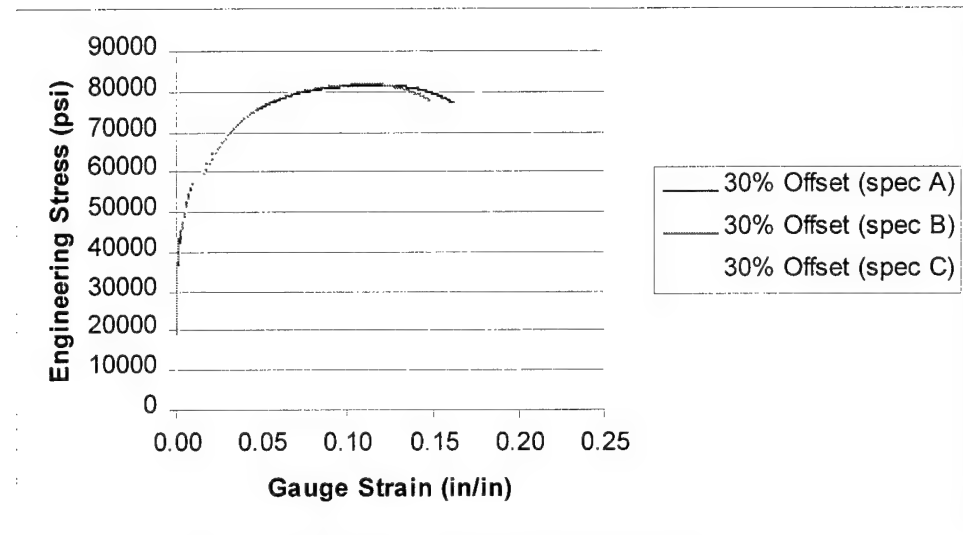
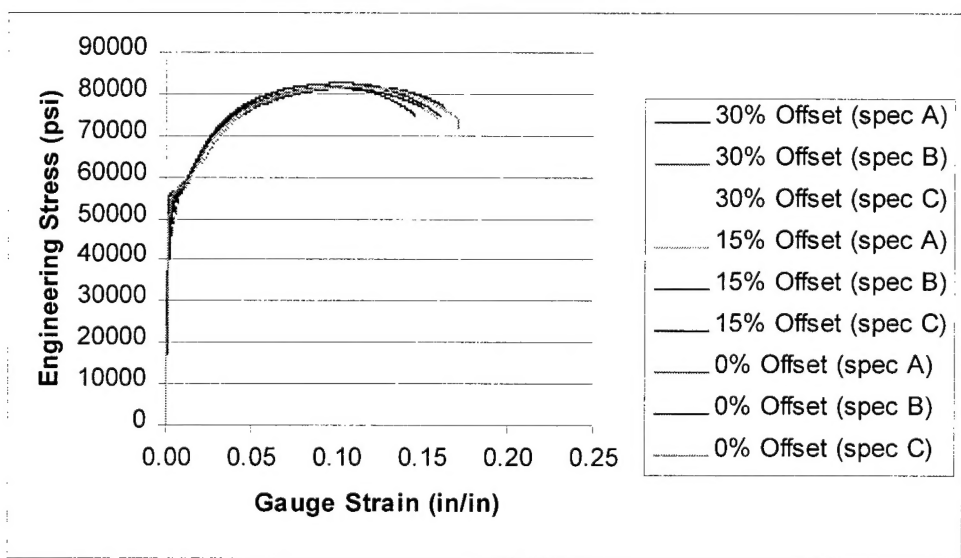
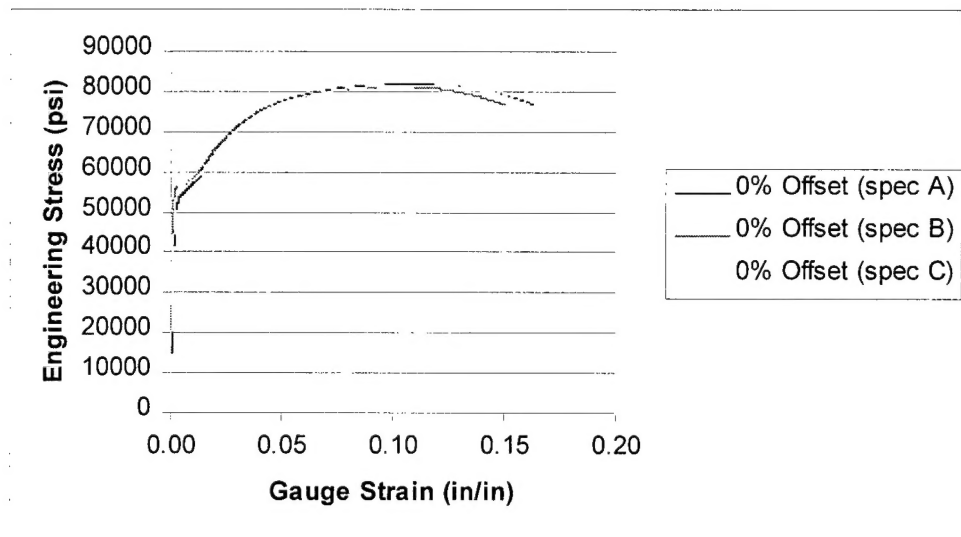


Figure 22. 0% offset case

APPENDIX H EH-36 ENGINEERING STRESS vs. GAUGE STRAIN





APPENDIX I AL6XN ENGINEERING STRESS vs. GAUGE STRAIN

